AGE (2005) 27: 75–90
DOI 10.1007/s11357-005-4131-3

Research article

Phenotype screening for genetically determined age-onset disorders and increased longevity in ENU-mutagenized mice

Dabney K. Johnson[1,*], Eugene M. Rinchik[1], Naima Moustaid-Moussa[2], Darla R. Miller[1], Robert W. Williams[3], Edward J. Michaud[1], Monica M. Jablonski[3], Andrea Elberger[3], Kristen Hamre[3], Richard Smeyne[4], Elissa Chesler[3] & Daniel Goldowitz[3]
[1]*Life Sciences Division, Oak Ridge National Laboratory, P.O. Box 2008, Oak Ridge, TN 37831-6420, USA;* [2]*Department of Nutrition, University of Tennessee, Knoxville, TN 37996, USA;* [3]*Department of Anatomy and Neurobiology, University of Tennessee Health Sciences Center, Memphis, TN 38163, USA;* [4]*St. Jude Children's Research Hospital, Memphis, TN 38105, USA; *Author for correspondence (e-mail: johnsondk@ornl.gov; fax: +1-865-574-1283)*

Received 6 August 2004; accepted in revised form 1 November 2004

Key words: age-onset, ENU mutations, longevity, neurological disorders, phenotype-screening

Abstract

With the goal of discovering genes that contribute to late-onset neurological and ocular disorders and also genes that extend the healthy life span in mammals, we are phenotyping mice carrying new mutations induced by the chemical *N*-ethyl-*N*-nitrosourea (ENU). The phenotyping plan includes basic behavioral, neurohistological, and vision testing in sibling cohorts of mice aged to 18 months, and then evaluation for markers of growth trajectory and stress response in these same cohorts aged up to 28 months. Statistical outliers are identified by comparison to test results of similar aged cohorts, and potential mutants are recovered for re-aging to confirm heritability of the phenotype.

Introduction

The Tennessee Mouse Genome Consortium (TMGC), a scientific and administrative association of public (The University of Tennessee, East Tennessee State University, University of Memphis) and private (Meharry Medical College, Vanderbilt University) universities, a clinical research institution (St. Jude Children's Research Hospital), and a national laboratory (Oak Ridge National Laboratory) was formed in 1998 for joint research projects utilizing statewide clinical, academic, and basic research expertise. Awarded a UO1 grant (UO1 MH61971) from the National Institute of Mental Health in 1999 for mutagenesis and phenotype-screening for disorders in behavior and the central nervous system, the TMGC effort includes an aging-colony core component designed to discover both lifespan-compromising and lifespan-extending single-gene recessive mutations. A genetics strategy was designed to produce enough genetically similar mice from each breeding pedigree to allow multi-site screening and sufficient statistical power for identification of outliers manifesting abnormalities in these variable and complex traits. The goal of the phenotyping protocols for all TMGC cores (general behavior, social behavior, drug related behavior, alcohol sensitivity, hearing, eye, neurohistology, epilepsy, and aging) is to perform primary screening tests that identify, and then validate as heritable, abnormal phenotypes resulting from the induction of new gene mutations.

We have learned many times throughout the gene-cloning years that biology is full of surprises, and that the set of functions associated with any gene throughout the life of the organism can be unpredictable. Because of this, the TMGC chose to take a

phenotype-driven approach to this project, in which large numbers of mice carrying induced point mutations can be screened for phenotypes of interest without any prior knowledge of which genes or genetic pathways may determine the traits. The only induced mutations that count in this approach are the ones ascertained because they cause an abnormal phenotype. The downside to this approach is that after a phenotype of interest is discovered and confirmed, it remains to map and confirm the gene that has been altered to produce the phenotype. However, given our high-throughput methods for identifying ENU-induced single-basepair changes in the DNA of coding sequences of genes that may be likely candidates, our chances of associating gene with phenotype are reasonable. Phenotype-driven gene discovery can also be approached using mouse mapping strain sets, like recombinant inbred strains, that offer natural genetic variants (single-basepair changes or other polymorphisms) that confer phenotypic differences amenable to measurement. The power of the currently available mapping strains for associating gene with phenotype is severely limited by the numbers of strains available in mapping sets; this difficulty will be overcome with the generation of the Collaborative Cross, a complex-trait community effort to breed 1000 recombinant inbred strains from eight genetically diverse inbred strains (Vogel 2003; The Complex Trait Consortium 2004; de Haan and Williams 2005).

The mutagen is *N*-ethyl-*N*-nitrosourea (ENU), a chemical that induces mostly point mutations in mouse spermatogonial stem cells. Each pedigree descends from one mutagenized male gamete, and the genotype of that gamete is tracked through the breeding scheme by following either a visible phenotypic marker or a set of DNA markers. Mice for screening are generated both at the Oak Ridge National Laboratory (ORNL) and at The University of Tennessee Health Sciences Center (UTHSC) in Memphis. In the case of ORNL, the mutagenized chromosome is brought to homozygosity in the third generation opposite a "balancer" chromosome with a large chromosomal inversion that includes both a dominant lethal mutation and a recessive mutation that confers a visually identifiable phenotype. Mice of the genotype that is homozygous for the mutagenized G_0 grandparental chromosome constitute the "test class," or the genotypic class that should manifest any abnormal recessive phenotypes caused by a new ENU-induced mutation in the region of the grandparental chromosome "balanced" by the chromosomal inversion. This third generation also includes mice that are heterozygous for the mutagenized grandparental chromosome and thus are carriers for any newly induced mutation that might be a developmental or genetic lethal. These G_3 heterozygous carriers would manifest new mutant phenotypes only if the new mutation were dominant (in which case the G_1 mice in the breeding strategy would also manifest the dominant phenotype). For the purposes of high throughput for primary screening by the TMGC, only the "test-class" mice are assayed for abnormal phenotypes; phenotypic effects of new mutations in other genotypes are tested later during confirmation of heritability.

In the case of mice produced at UTHSC, the mutagenized males are consomic for a PWK or A/J chromosome introgressed into the C57BL/6J background. G_3 mice homozygous for new mutations in the PWK or A/J G_0 grandparental "target" chromosome are identified by microsatellite genotyping, and constitute the "test class" as above. For the aging core, four males and four females of the "test class" are group-housed at weaning to await behavioral screening at 18 months for age-onset neurological disorders and screening at 19–24 months for factors (related to growth and stress response) thought to be predictive of longevity. All mice are weighed at least monthly beginning at weaning or earlier, and after the final screening are aged to 28 months or longer.

Three and a half years into this five-year project, we have aged 325 pedigrees to 18 months and 202 pedigrees to 28 months or more. We have screened the 18-month-old mice for abnormalities in general central nervous system function (locomotor activity, startle reflex, habituation to startle, and prepulse inhibition of the startle reflex, learning and memory as assessed by fear conditioning, nociception), neurohistology, and eye morphology. We have screened the 19-month or older mice for body weight, blood glucose, leptin, insulin, insulin-like growth factor, corticosterone, and ability to maintain body temperature in the cold. Many pedigrees remain to be screened for these age-related phenotypes, and we have identified putative mutants ("putants") for most screens. Pedigrees are being recovered for confirmation of heritability of the ascertained phenotype by breeding old males or by performing intracytoplas-

mic sperm injection (ICSI) using sperm routinely frozen from young males from the pedigree.

Materials and methods

Mice. Mice for aging were generated using chromosomal inversions of two mouse chromosomes (Chr), 7 and 15 (ORNL) and consomics for Chr 14 and 19 (UTHSC). Table 1 shows the strains that were mutagenized and the mating partners, the dose of ENU, the markers followed (visually or by genotyping), and additional information about the genetic backgrounds. The strategy for Chr 15 and for the use of chromosomal inversions applicable to these experiments have been described (Rinchik 2000).

For Chr 7, the mutagenized strain was the non-inbred D7R75M stock (*a*/*a*; p^{7R}/p^{7R}). The p^{7R} mutation is the visible marker (fur color) making a coat color that is intermediate between wild-type and p. The chromosome carrying the p^x mutation is the one that also carries the new ENU mutations, so we can follow the location of the ENU mutations by following the p^x marker. In addition, mice that are p^x/p^x in coat color are the test class; absence of this color class means that the new recessive mutation is an embryonic lethal.

The Chr-7 region corresponding to the "target region" for mutagenesis in this screen is predominantly of C3H origin, based on an SSLP survey of a number of p^{7R}/p^{7R} G_3 or greater mice (see below), although it could be of B6 origin in any one mouse in any one pedigree. Mice homozygous for p^{7R} are darker in color than are p^{7R}/p, or p^{7R}/In(7)*p*4Rl animals. The prenatally recessive-lethal ln(7)*p*4Rl inversion (Russell et al. 1995) was used as a dominantly marked, recessive-lethal "balancer" to follow mutagenized chromosomes so that the "test class" homozygous for the mutagenized chromosome could be visually detected in G_3. The proximal breakpoint of the inversion maps within the *p* gene itself, while the distal breakpoint maps some 20 cM distal, in the vicinity of *pid*, just proximal to *Myo7a*. The lethal In(7)*p*4Rl inversion was maintained by crosses of p^{7R}/In(7)*p*4Rl heterozygotes to p^{7R}/p^{7R} mates. Non-inbred D7R75M p^{7R}/p^{7R} G_0 males were treated with ENU and were mated to p^{7R}/In(7)*p*4Rl females. Light-colored G_1 males [p^{7R} *m*/In(7)*p*4Rl +, where *m* is a newly induced, linked ENU mutation] were crossed to females of the genotype + $Tyr^{c\text{-}ch}$/In(7)*p*4Rl+. The resulting G_2 generation manifests two phenotypic categories, wild-type and light-colored [In(7)*p*4Rl/In(7)*p*4Rl embryos die before implantation]. Light-colored G_2 males and females [p^{7R} *m*/In(7)*p*4Rl +] were intercrossed to yield a G_3 generation with two surviving genotypic classes: p^{7R} *m*/In(7)*p*4Rl +, light-colored carriers of the ENU-mutagenized chromosome; and p^{7R} *m*/p^{7R} *m*, dark-colored and homozygous for the mutagenized chromosome. These darker animals comprise the test class, in which any new recessive phenotype resulting from a mutation induced in mid Chr 7 would be found. The absence of mice of the test-class color indicated that the newly induced mutation was embryonic lethal.

For Chr 15. the mutagenized strain was C3H/Rl, and the balancer inversion, congenic on C3H/Rl, is called 4R250M and carries the dominant-lethal marker hairy ears (*Eh*). The ENU-treated G_0 males were mated to *Eh*/+ females, and the G_1 males or females (*Eh* ++/+ *m* +, where *m* indicates a newly induced mutation) were crossed to *Eh* ++/++ *Crld*, This latter stock, also congenic on C3H/Rl, segregates both the *Eh* inversion and *Caraculoid* (*Crld*), a dominant *Caracol*-like mutation that does not re-

Table 1. Strains, dosages of ENU, mating partners, and phenotype/genotype markers for mutagenized mice undergoing screening.

Experiment	Chr	ENU, mg/kg (no. of males)	Injected strain	G_0 female	Markers
TNA	Distal 15	4 × 50 (37)	C3H/Rl	C3H/Rl-*Eh*/+	Hairy ears
TNB	Distal 15	3 × 50 (44)	C3H/Rl	C3H/Rl-*Eh*/+	Hairy ears
TNC	Distal 15	2 × 50 (42)	C3H/Rl	C3H/Rl-*Eh*/+	Hairy ears
TND	Mid 7	1 × 200 (30)	D7R75M	In(7)p4Rl/+	Coat color
TNP	Mid 7	1 × 125 (42)	D7R75M	In(7)p4Rl/+	Coat color
CH14	14	1 × 150 (27)	C57BL/6J-Chr 14^{A}/NaJ	C57BL/6J	D14Mit98, 133, 260, 115, 226
CH19	19	1 × 150 (40)	C57BL/6J-Chr 19^{PWK}	C57BL/6J	D19Mit59, 86, 10, 137

C3H/Rl mice are *rd*/*rd* and are blind. D7R75M segregates *rd*.

combine with the Eh inversion. G_2 mice with the *Eh* (but not the *Crld*) phenotype (*Eh* + +/+ *m* +) were then intercrossed to generate test-class mice (+ *m* +/+ *m* +) for screening and heterozygotes (*Eh* + +/+ *m* +) as carriers of lethals (recognized as the absence of mice with normal ears).

For chromosomes 14 and 19, males from consomic strains C57BL/6J–Chr14^{A}/Na/J and C57BL/6J–Chr 19^{PWK} were mutagenized and mated to C57BL/6J females. This strategy has been described (Williams 1999). G_1 offspring that maintained whole chromosomes 14 or 19 (from A/J or PWK) were selected using the microsatellite markers listed in Table 1 and intercrossed. Again, G_2 that maintained whole chromosomes 14 or 19 (from A/J) were selected using the microsatellite markers listed in Table 1 and intercrossed to form the G_3 test class.

Mutagenesis. Males were given a single or multiple weekly intraperitoneal injections of ENU, prepared as previously described Russell et al. (1979) at doses given in Table 1. ENU was obtained from Sigma (St. Louis, MO). From Table 1, the mice being screened that have reached at least 18 months in the aging colony at this writing are from experiments TNA, TNB, TNC, TND, TNP, CH14, and CH19. After fertility returned, the males were mated to experiment-appropriate females as outlined above.

Test-class animals in each pedigree were observed at weaning for obvious neuromuscular and/or behavioral phenotypes, size differences, and other visible phenotypes. Mutant phenotypes should be apparent only in the test-class; mutant phenotypes appearing in other genotypic classes of G_3 mice, but not in any of their parents, predict an unlinked recessive mutation. At ORNL, the test-class mice were weighed at two weeks postnatal as whole litters and at six weeks as individuals; each mouse at both ORNL and UTHSC is weighed at weaning, at eight weeks of age, and then monthly thereafter. The absence of test-class animals in 15 or more animals of any pedigree (one-third expected, $P < 0.002$), identified pedigrees in which homozygosity for that mutagenized chromosome segment is pre- or neonatally lethal due to mutations in essential developmental functions. Breeding stocks were established from any pedigrees with visible or lethal mutations; all mutations, including lethal or otherwise detrimental ones, were propagated from intercrossing the G_2 siblings heterozygous for the ENU mutation and the "balancer" inversion. For each pedigree, two young males were sacrificed for cryopreservation of sperm, one young female underwent a microCT scan, and brain, liver, spleen, kidney, tail, ovary, and testis were archived by freezing.

For all pedigrees with an apparently normal test class, four males and four females were set aside in group housing at weaning, and aged to 18 months. Each mouse was weighed at weaning, at six weeks, and then monthly, and examined quarterly by an experienced technician for visible abnormalities, including a click-box test for hearing. At 18 months, two males and two females went through a general behavior-test regime, and one male and one female were sent to UTHSC for neurohistology (leaving six mice to age to 28 months or more). In recent months, these two aged mice from each pedigree also underwent eye examination prior to sacrifice for neurohistology. Detailed protocols for all tests and stains may be found at http://www.tnmouse.org, but briefly, each of the four mice from each pedigree was given a 20-min open-field activity test in a Hamilton–Kinder chamber, concurrent assessments of acoustic startle, startle habituation, and prepulse inhibition of startle reflex in a Hamilton–Kinder startle chamber, cued and contextual fear conditioning (electric shock to the foot pads), and a 52 °C hotplate test for nociception. For neurohistological examination, one mouse was taken for perfusion fixation 1 hour after an i.p. injection of bromo-deoxyuridine (BrdU) to label mitotically active cells and another for fresh taking of the brain which was weighed and frozen in isopentane cooled to −80 °C. These brains were then processed for a series of histological stains to highlight specific aspects of the neuropil including neurons, glia, transmitter-specific cell bodies and projections, and proliferatively active cells.

For the ocular examination, the anterior and posterior segments of the eyes of one mouse aged to 18 months from each pedigree were evaluated using a slitlamp biomicroscope and an indirect ophthalmoscope. Images were also taken of the posterior segment with a fundus camera. Eyes were then processed to assess for variations in ocular structure and to highlight specific retinal markers.

Recovery of potentially mutant pedigrees. When possible, putants are recovered via breeding of aged males to young wild-type females of appropriate genetic strains. For example, for putants on Chr 15, aged homozygous-mutant males are bred to C3H/Rl

females to generate F_1 heterozygotes, which are then intercrossed to generate an F_2 population for aging, phenotyping, and confirmation of heritability. Twenty-five percent of aged F_2s should manifest a recessive mutant phenotype that is heritable.

If the aged males do not breed, the pedigree is recovered via intracytoplasmic sperm injection (ICSI) using sperm cryopreserved from a young homozygous-mutant male of the pedigree. Donor eggs are derived by superovulation of females of the appropriate genetic background to generate F_1 progeny.

The collection and cryopreservation of spermatozoa, superovulation of female mice, collection of oocytes, ICSI, preimplantation culture conditions, and transfer of two-cell stage embryos into foster mothers were performed essentially as described (Kimura and Yanagimachi 1999; Kawase et al. 2001; Szczygiel et al. 2002 and references therein). Briefly, sperm were obtained from the epididymides and vas deferentia of each mouse in 1 ml of cryoprotectant (18% raffinose, 3% nonfat dried milk in distilled water) and distributed into straws in aliquots of 100 μl. The straws were sealed, suspended in the vapor phase of liquid nitrogen in a styrofoam cooler for 10 min prior to immersion and storage in liquid nitrogen. Mice were induced to superovulate with intraperitoneal injections of PMSG (5 IU), followed 48 h later with HCG (5 IU). Oviducts were removed 12–15 hr after the injection of HCG, and the cumulus cell-oocyte masses were released from the ampullae into 0.1% hyaluronidase to obtain oocytes free of cumulus cells for ICSI. Prior to ICSI, one straw containing cryopreserved sperm was quickly thawed in a 37 °C water bath. The sperm was expelled from the straw, thoroughly washed in saline solution to remove cryoprotectant, centrifuged, resuspended in 300 μl of saline and distributed into aliquots of 15 μl. One aliquot was used for ICSI and the remaining aliquots were refrozen in liquid nitrogen for subsequent days of ICSI. The sperm aliquot used for ICSI was placed in an equal amount of M2 media containing 16% polyvinyl pyrrolidone. ICSI was performed with a Prime Tech piezoelectric microinjection system (PMM-150FU), Eppendorf NK-2 micromanipulators, and a Nikon TMD microscope. Single sperm heads were injected into each oocyte. Fertilized eggs were cultured overnight in KSOM for the development of two-cell stage embryos, which were transferred into the oviducts of pseudopregnant ICR recipients. All experiments involving mice in this study were conducted under approved Institutional Animal Care and Use Committee protocols.

Screens being performed in the aging colony for stress and growth parameters

Body weight. Body weights are taken at two weeks postnatal (entire litter), at weaning, at six weeks of age, at eight weeks of age, and then monthly thereafter to 28 months of age.

Cold challenge. Cold challenge to the ability to maintain core temperature is used to screen for energy-balance mutations and for stress resistance. For the cold-room challenge, mice are placed at 4 °C, in individual cages, and the rectal temperature of each mouse is taken with a rapid-read digital thermometer at 30-min intervals for up to 2 h. Normal mice maintain rectal temperature efficiently for the entire 2 h at 4 °C, whereas mice with energy-balance defects will lose, and not be able to regain, a few degrees (Dr Streamson Chua, Columbia University, personal communication).

Measurement of IGF-1, corticosterone, insulin, leptin, and glucose. Mice that have been through the cold challenge are tested for these hormones. Mice are bled no sooner than one week after the cold challenge. Blood is drawn by nicking the large vein at the base of the tail of a lightly restrained and warmed mouse, and collecting drops of whole blood in microtainer tubes. The samples are centrifuged and serum is collected. The serum is aliquoted that same day and kept at −80 °C until analysis. Collection is done late in the afternoon from unfasted mice.

(a) *Glucose* (mg/dl): A drop of whole blood is analyzed using a One Touch Profile glucometer.
(b) *IGF-1* (ng/dl): Serum samples are analyzed at the Jackson Laboratory by the Cliff Rosen (MECORE Laboratory at St. Joseph Hospital, Maine) group in order to ensure comparability to similar samples being assayed by Dr. James Nelson of the University of Texas Health Sciences Center at San Antonio.
(c) *Corticosterone* (ng/dl): Serum aliquots are shipped to Dr. Nelson for analysis.
(d) *Insulin* (ng/dl): Insulin levels are measured in the laboratory of Dr. Naima Moustaid-Moussa, De-

partment of Nutrition, The University of Tennessee at Knoxville) using 1–5 μl of serum, using the Ultrasensitive Rat Insulin ELISA Kit (with mouse insulin standards) obtained from CRYSTAL CHEM INC. The same kit is used by the Jackson Laboratory for their mutagenesis screens.

(e) *Leptin* (ng/dl): Leptin levels are measured in Dr. Moustaid-Moussa's laboratory using 1–5 μl of serum, using the Mouse Leptin ELISA kit obtained from Crystal Chem Inc. The same kit is used by the Jackson Laboratory for their mutagenesis screens.

Screens being performed in the aging colony for neurohistological abnormalities

Two mice from each pedigree are processed for examination using neurohistological stains. One mouse is decapitated and the brain and eyes weighed. The brain tissue is then dipped into room temperature isopentane (2-methylbutane) and the brains are cut midsagittally, placed on the cut surface, and quick-frozen in precooled isopentane (placed on dry ice for at least 30 min). Immediately after brain freezing the whole eyes are removed and frozen. Care is taken to minimize the time between decapitation and freezing (usually around 2.4–3.2 min) The tissues are then placed in 2.0-ml cryo-vials on dry ice for 15 min, then stored at −80 °C. One half of each brain and one whole eye are mounted together (side by side, in the sagittal plane) using refrigerated TBS Tissue Freezing Medium on a room temperature cryostat chuck placed on dry ice. The chuck containing the mounted tissue is then allowed to equilibrate in the cryostat at −18 °C for 20 min and the tissue then cut into 20-μm sections and stored at −80 °C. until ready for staining. A series of 10 stains is carried out on the fresh frozen material:

1. Cell bodies and cytoarchitectonics are demonstrated using Cresyl violet (0.03%).
2. Astroglia are highlighted using antiglial fibrillary acidic protein (GFAP) immunocytochemistry (Immunon 460740, raised in rabbit).
3. The energy state and mitochondrial activity are highlighted using cytochrome oxidase histochemistry (tissue is stained using a filtered solution of 24 mg Cytochrome C (Sigma C-2506), 45 mg of Diaminobenzidine (Sigma D-3001), and 3 g sucrose in 60 ml 0.01 M KPBS (pH 7.40) for 70 min in a 35 °C water bath, gently shaken and protected from light.
4. Myelinated axons are visualized using either a stain with 2% OsO_4/5% sucrose for 20 min or Luxol Fast Blue.
5. Proliferating cells are visualized using an antibody to histone H3 (INFO).
6. Cholinergic innervation and cell bodies are highlighted using a histochemical stain for acetylcholinesterase (AChE). The staining protocol is as follows; solution A: add 10 ml 0.1 M Na acetate (pH 5.3) to 7 ml dH_2O + 0.8 ml Cu glycine (3.75 g glycine + 1.6 g anhydrous $CuSO_4$ in 100 ml dH_2O). Solution B: dissolve 29 mg Acetylthiocholine Iodide (Sigma A-5751) in 1.5 ml dH_2O and vortex, then add 0.5 ml of 0.1 M $CuSO_4$ and vortex quickly (to prevent too much precipitate), then centrifuge at 2000 rpm for 10 min. Solution C: dissolve one 25-mg tablet of Promethazine (available at most pharmacies) in 10 ml dH_2O (mix ~30 min on a stir plate, protected from light) and filter into foil-covered vial. Combine solution A with the supernatant from solution B to make solution D, then add 0.5 ml of solution C per 20 ml of solution D. The slides are then incubated for *at least* 6 h in a Coplin jar with slow rotation (protected from light), developed in 1% $(NH_4)_2S$ + aq. (Fisher A705-250) for 90 s, and rinsed in dH_2O.
7. Neurons are selectively highlighted using immunocytochemistry for anti-NeuN (Chemicon MAB377, raised in mouse; used at 1:1000).
8. Neuropathological alterations associated with the ubiquitination of proteins are examined using anti-ubiquitin immunostaining to highlight neuronal pathology.
9. Noradrenerigic and dopaminergic neurons and fibers are stained using anti tyrosine hydroxylase immunocytochemistry.
10. The mossy fiber projection from the dentate gyrus to the hippocampus is highlighted with the Timm's stain for heavy metals. Other terminal fields are also highlighted with this stain.

All slides are then dehydrated, differentiated, and coverslips are applied with Permount.

The second mouse is administered BrdU (Sigma, 0.1 ml/30 g body weight or 50 μg/kg) and sacrificed

one hour later using perfusion fixation with 1:3 acetic acid/95% ethanol. The brains and eyes are removed and embedded into paraffin and sectioned at 8-μm thickness. Tissue is mounted on slides and typically stained for Cresyl violet, anti-GFAP, and anti-BrdU (Becton-Dickinson 347580, raised in mouse; used at 1:25) to test the reproducibility of results in the fresh frozen material for cells, glia, and cell proliferation. A fourth set of sections are stained for anti-Calbindin immunocytochemistry. Three stains are performed on sections from the perfusion-fixed brain using a pretreatment protocol consisting of 10 min in a 0.04% Pepsin (Sigma P-6887) in 1 N HCl solution, followed by rinses in 2× SSC at 80 °C for 5 min, 70% ETOH at 60 °C for 2 min, 0.1 M PBS at room temperature for 3 min, and in 0.1 M PBS + 1% H_2O_2 for 3 min. Slides are then immunocytochemically stained with anti-BrdU (Becton-Dickinson 347580, raised in mouse; used at 1:25), counterstained with 0.03% Cresyl violet for 20 min.

Screens being performed in the aging colony for eye abnormalities

To evaluate the ocular phenotype of each 18-month-old mouse (one mouse per pedigree), we utilized our protocols as previously described (Semenova et al. 2003; Martin et al. 2004). Briefly, the anterior segment of the eye (i.e., cornea and lens) was examined using a slit lamp biomicroscope (Carl Zeiss, Germany). Images of these structures were recorded with a Canon GL1 digital video camera (Canon USA, Inc., Lake Success, NY) via a video adapter (Transamerican Technology International, San Ramon, CA). Pupils of mice lightly anesthetized with an intraperitoneal injection of Avertin were dilated with Cyclomydril (Alcon Pharmaceuticals, Fort Worth, TX). The fundus was examined by indirect ophthalmoscopy and photographs were taken with a Kowa Genesis small animal fundus camera (Genesis; Kowa, Torrance, CA) with the assistance of a 90-D condensing lens (Volk Optical, Mentor, OH) as described previously.

Paraffin sections of both eyes from each mouse were stained with Hemotoxylin and eosin using standard protocols. Additional slides were immunostained using antiglial fibrillary acidic protein (GFAP) antibodies (Thermo Electron Corporation 460740 at 6 drops per 1000 μl) and anti-calbindin D-28K (Chemicon AB1778 at 1:250 dilution). Immunoreaction products were visualized using a Vectorstain kit (Vector Laboratories, Inc., Burlingame, CA). Slides were examined on a Nikon Eclipse E800 microscope equipped with Sensys Color Camera (Photometrics, Tucson, AZ) and images were collected using MetaMorph Imaging System software (Universal Imaging, West Chester, PA).

Data analysis

Data from each of these tests are entered into Mutrack, the TMGC database at http://www.tnmouse.org, and Mutrack performs statistical analyses to identify outlier pedigrees for each screen. If the pedigree mean is >1.65 SD from the population mean (with 25% trimming and at least 10 pedigrees tested), and the pattern of the data points for each mouse relative to the mean is meaningful (see plots below), a pedigree is declared to be a "putant" (putative mutant). "Putancy" cues retesting, which for the aging pedigrees means retest of already-tested mice and testing of any remaining aging mice. If retest results confirm the outlier status of the pedigree, that pedigree becomes a "cutant" (confirmed putant). An aging pedigree can become a mutant (heritability confirmed) only when the pedigree is recovered from breeding old males or from intracytoplasmic sperm injection using frozen sperm and re-aged for testing.

Data may be viewed on Mutrack at http://www2.tnmouse.org/mutrack/index/php and logging on using TMGC as the Username and Read as the password. Under Mutrack Statistics, click on Statistics Homepage, then under Navigate, click on SAS Stats. Under Statistics Tools, click on Weekly Update. The Weekly Update for each screening domain is a table that gives the pedigree and the data field(s) for any outliers (>1.65 SD). Going back, under Statistics Tools, click on Test Tables and find the data for the individual pedigree and data field of choice (check a project, i.e. TND, then select a data field from the pull-down menu. The "See graph" link at the top of the test table will show data-point plots for each individual mouse in all pedigrees tested in that project/family. Weight data ("Aging Weights" under both Weekly Update and Test Table) and growth/stress screens on aging mice ("Physiology" under both Weekly Update and Test Table) are updated each week.

Results: potential mutants for behavior, neurohistology, eye

The pedigrees in Table 2, potentially mutant for behavior tests performed at 18 months of age, were normal on the given test as young mice, suggesting an age-onset abnormality.

Neurohistology

Aged brains from 97 eighteen-month-old pedigrees have thus far been examined. All sections are uniformly processed with the same concentration of antibody, fixation protocol, thickness of tissue, and these findings are very reproducible in all of the aged pedigrees we have examined compared to all of the young examined. Thus, we conclude that the differences seen with each stain are caused by age-associated neuroanatomical changes, and that we will be able to detect age-associated abnormalities against this background of normal changes.

However, since we sample only 2 brains from each of these lines (so that they may age for another 10 months), these pedigrees cannot be unequivocally assigned as "normal" or "mutant". The idea is that any strikingly mutant lines will be designated for reexamination after recovery and re-aging. To date, we have identified 14 putative mutant lines with none having a phenotype that would, by itself, command the effort to recreate and age the line. Interestingly, however, one pedigree that may be an outlier for brain weight (n = only 2), 253TNB, is also an outlier for body temperature (see below in Figure 2) in the extra-ager screen. It will be interesting, however, to see how all of these putants look in the remaining cohort of their pedigree at 28 months. What we have identified is a set of neuroanatomical abnormalities that are associated with the aged brain. These include a dramatically decreased number of proliferating cells (indicated by arrows in Figure 1) in the rostral migratory stream (RMS) and dentate gyrus as seen with anti-BrdU immunocytochemistry (arrows in BrdU) panel. Likewise, there are reduced numbers of anti-histone H3 positive cells in these areas; H3 and BrdU staining suggest a normal, age-related reduction in the amount of cell proliferation in the these areas. There also is an increase in ectopically placed histone H3-positive cells in regions that are not identified as normally proliferative including the striatum and various areas of cortex (data not shown). This may represent cells with DNA damage and repair. An increase in GFAP immunoreactivity is also a hallmark of the aged brain, and this is particularly obvious in the thalamus. Finally, there is a variable but obvious drop out of Calbindin-positive Purkinje cells in the aged cerebellum. These attributes of the 18-month-old brain, compared to the 10-week-old brain, are illustrated in the Figure 1.

Ocular phenotypes

The ocular phenotypes of 35 eighteen-month-old pedigrees have been evaluated. Upon immunohistochemical evaluation, all pedigrees had an increase in GFAP immunoreactivity, similar to the increase noted in the brains of aged mice. Of the 35 lines examined (one mouse per line), five pedigrees were part of the TNA/TNB/TNC projects and were therefore homozygous for mutations in *retinal degeneration* (*rd*, *Pdeb* – the *rd* mutation is carried by the inbred strain C3H, and so is segregating in the background as a preexisting mutation in some of the mice being screened). These mice had severely degenerated retinas that were obvious on both the ophthalmic and histological exams. Ten pedigrees had a cataract that precluded

Table 2. Pedigrees potentially mutant for behavior tests performed at 18 months of age.

Putant pedigree	Mutant phenotype	Specific test (s)	Outlier status
12TNJ	Learning/Memory	Context fear	2.64 SD
23TND	Hearing	Click box	All apparently deaf
11TNB	Locomotor activity	Rearing	−1.96 SD
		Total distance	−2.07 SD
66TNP	Acoustic startle response	Prepulse inhibition	70 dB, 4.44 SD
			80 dB, 3.66 SD
			85 dB, 3.96 SD

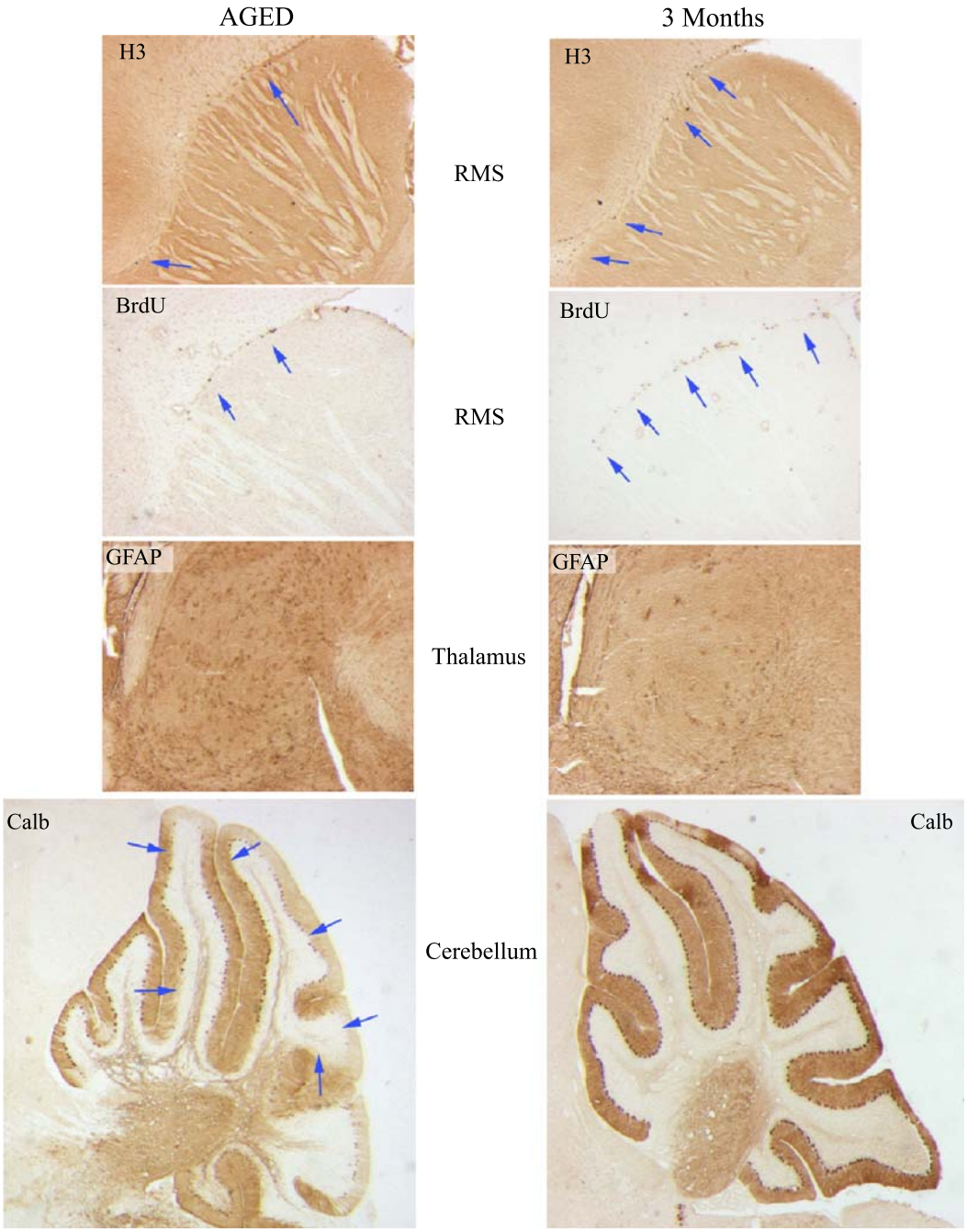

Figure 1. Comparison of Calbindin stained images of 10-week-old and 18-month-old cerebellum. Immunocytochemical images that highlight some of the consistent findings in the 18-month-old brain in comparison with the 10-week-old brain. Arrows in the top panel (H3) point to H3-positive (and therefore, proliferating) cells in the rostral migratory stream (RMS); likewise, arrows in the BrdU panel also indicate proliferating cells in the RMS as visualized by the uptake of BrdU. In the glial fibrillary acidic protein (GFAP) panel, amount of immunopositivity is compared in the thalamus between young and aged brains. Anti-calbindin antibody lights up a variety of cell types, including cortical neurons and cerebellar Purkinje cells. To the right is shown the normal 10-week-old phenotype of numerous proliferating cells in the RMS, a lightly populated glial area in the thalamus and a full expression of Calbindin in the Purkinje cells of the cerebellum. In contrast, there is a greatly reduced number of proliferating cells in the RMS, much greater occupation of thalamus by glial processes and areas in the cerebellum that are devoid of calbindin immunoreactivity.

the evaluation of the fundus; the cataracts were not graded, and were not considered further as abnormalities resulting from new mutations. The corneas of two independent pedigrees were opaque to varying degrees, thus also limiting our visibility of the fundus in the intact eye. In all of these lines, our evaluation of the retina was limited to the histological and immunohistochemical evaluation of the eye. In nine TND and TNP pedigrees, the fundus was slightly pale at a subretinal level, which is suggestive of loss of pigmentation of the retinal pigmented epithelium (RPE) and/or choroid. This finding was not present in all TND and TNP pedigrees; four other mice had normal pigmentation levels of the fundus.

The 44TNJ pedigree, a pedigree that is a well-characterized mutant line in 8- to 10-week-old mice, was the most severely affected pedigree in the aged mice that we examined. In this line, an examination of the fundus was precluded due to a cloudy cornea. Histological evaluation revealed that the outer nuclear layer containing photoreceptor nuclei was thinner, suggestive of photoreceptor cell death. The inner and outer segments of the remaining photoreceptors were shortened compared to other aged mice. Moreover, the continuity of the outer plexiform layer was disrupted, as was the calbindin-positive staining of the horizontal cell processes that should be located in this plexiform layer. The cell bodies of the horizontal cells also had significantly lighter calbindin-positive staining than those of other aged mice. Retinas of the 44TNJ mouse were also very heavily stained by the anti-GFAP antibody.

Three other pedigrees (i.e., 73TND, 115TND and 117TNP) shared a common characteristic of having a normal histologic appearance of the retina, yet immunohistochemical analyses revealed an aberrantly light calbindin-positive staining of horizontal cells of the outer retina and a subtype of amacrine cells in the inner retina. This feature, although common in the Purkinje cells of the aged cerebellum, is not shared by the retinas of all aged mice. The 117TNP pedigree was also called as a mutant in 10-week-old mice for aberrant pigmentation patterns of the fundus. In the young mice, the calbindin positive staining patterns were normal, thus this feature appears to be age-related.

The final aberrant ocular phenotype of the aged mice occurred in the 163TNP pedigree. In this mouse, a ring-like pattern of subretinal depigmentation was present in the fundus examination. Retinal histology and immunohistochemical findings were normal in this pedigree, although there appeared to be some

Table 3. Aging putants for ocular phenotypes.

Putant pedigree	Mutant phenotype	Specific test (s)	Outlier status
73TND	Retinal immunolabeling patterns	Calbindin immunohistochemistry	Light calbindin-positive staining of horizontal cells and a subset of amacrine cells in inner retina
115TND	Retinal immunolabeling patterns	Calbindin immunohistochemistry	Light calbindin-positive staining of horizontal cells and a subset of amacrine cells in inner retina
117TNP	Retinal histology and immunolabeling patterns	Calbindin immunohistochemistry	Light calbindin-positive staining of horizontal cells and a subset of amacrine cells in inner retina
44TNJ	Retinal histology and immunolabeling patterns	Retinal structure; Calbindin immunohistochemistry; GFAP immunohistochemistry	Mislocated photoreceptor nuclei over photoreceptor outer and inner segments; Shortened photoreceptor inner and outer segments; Disrupted outer plexiform layer; Light calbindin-positive staining of horizontal cells and a subset of amacrine cells in inner retina; heavy GFAP immunolabeling of Müller cells
163TNP	Retinal histology and immunolabeling patterns; fundus examination	Fundus examination; subretinal structure	Separation of layers of the choroid; Depigmentation of fundus around optic nerve head

Table 4. Potential mutants for stress and growth parameters.

	Body wt.	Cort	IGF-1	Insulin	Leptin	Glucose	Cold stress
29TNA (n = 4)		2.67[a] SD					
92TNC (n = 4)			3.51 SD				−3.60 SD
60TNB (n = 4)						3.16 SD	
78TNA (n = 3)						−6.23 SD	
138TNA (n = 4)			3.62 SD	3.66 SD			
166TNC (n = 4)	Low wt.				−2.14[b]		
221TNB (n = 4)			2.39 SD				
253TNB (n = 3)							3.02 SD[c]
122TNP	Low wt.						
115TND (n = 2)		3.2 SD			6.65 SD		
248TNC (n = 8)							−4.21 SD at 90 min; −2.75 SD at 120 min

[a]Pedigrees are designated as outliers and thus potential mutants if the pedigree mean is >1.65 SD from the population mean (with 25% trimming and at least 10 pedigrees from the same experimental protocol (see Table 1) tested. The population used here for deriving the population mean is all other aged test-class mice from the same experiment.
[b]166TNC also has a z score of −2.79 for body weight at 25 months.
[c]253TNB has hyperthermic basal temperature (1.41 SD), is 3.02 SD at 30 min in the cold, 2.35 SD at 60 min in the cold, and 1.74 SD at 90 min in the cold.

separation or thinning of the layers of the choroid. Like the 44TNJ and 117TNP pedigrees, this line was called as a mutant pedigree in 10-week-old mice. The aberrant nature of this pedigree appeared to progress to include depigmentation of the fundus to the area surrounding the optic nerve head, a feature that was not present in the younger mutant mice. Potential ocular abnormalities are summarized in Table 3.

Potential mutants in the extra-aging colony

To date, 202 pedigrees have gone into extra aging beyond 18 months, and more are being added daily. Sixty pedigrees with six mice remaining have been screened for growth/stress indicators, and Table 4 shows potential mutants; all of these are in the process of recovery of young mice for re-aging, some by mating the aged males, and some by ICSI.

Figures 2–5 give examples of data analysis and presentation of representative potential mutants from Table 2. Inspection of the SAS plots in Figures 2–5 gives an idea of the degree of variance we experience for the growth/stress tests; this variance is limited enough that we can call statistical outliers as potential mutants for retest. Since we have not yet re-aged any of the potentially mutant pedigrees for retest, we cannot yet calculate our success rate in confirming mutants on these tests.

Recovery via the breeding of aged males, or by intracytoplasmic sperm injection (ISCI) using cryopreserved sperm.

Homozygous cutants from pedigrees 12TNJ (learning/memory), 23TND (hearing), 66TNP (acoustic startle response), and 122TNP (low body weight) are maintained live. Live heterozygotes for three cutant aging lines, 92TNC (cold challenge and IGF-1), 138TNA (IGF-1 and insulin), and 166TNC (low body weight and leptin) have been recovered via intracytoplasmic sperm injection into mouse oocytes using frozen sperm. For the remaining potential mutants, aged males are in matings at this time; ICSI will be used to recover lines for which the current matings are unsuccessful.

Discussion

The potential mutants illustrated in Tables 2–4 and Figures 2–5, although not yet proven heritable, represent single-gene mutations with pronounced effects on complex whole-organism phenotypes critical to normal CNS function, to homeostasis and maybe to longevity. From neurohistology screening, we are identifying a set of neuroanatomical changes that are associated with the aged brain in addition to our potential for discovering abnormal phenotypes resulting from induced new recessive mutations. We see

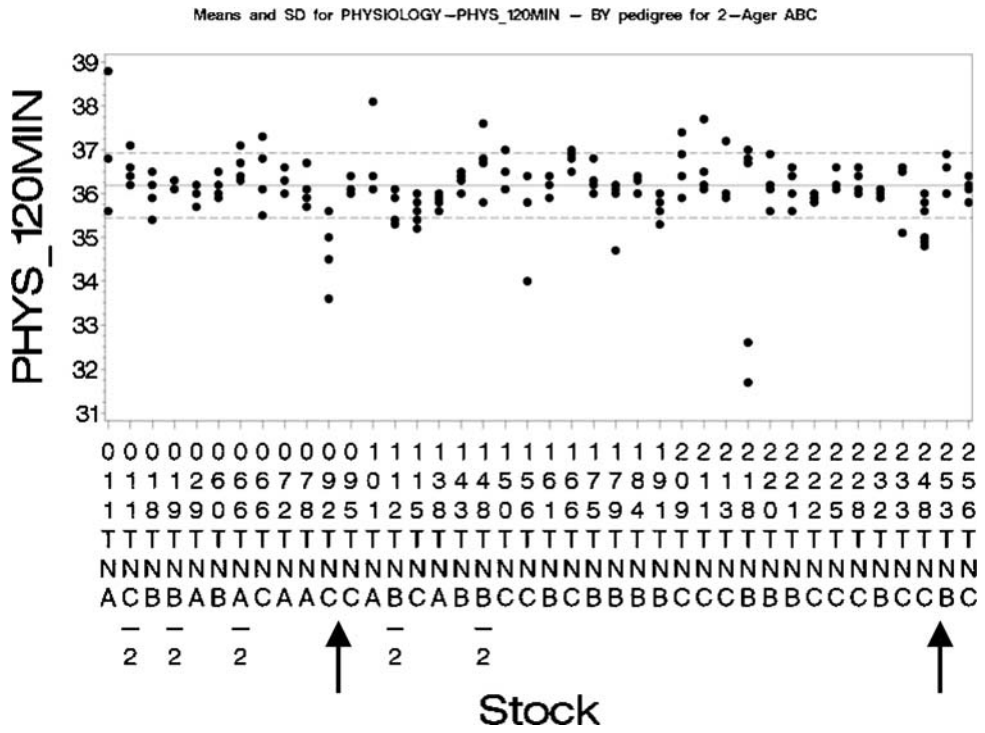

Figure 2. Body temperature of 92TNC after 120 min at 4 °C. Note also 253TNB, with temperature now down to normal at 120 min following consistent hyperthermia at earlier time points. SAS plot of data from cold challenge after 120 min at 4 °C from distal chromosome 15 families TNA, TNB, and TNC. Pedigrees are listed across the bottom, with data points from individual animals of the pedigree arranged vertically above each pedigree. The solid line at mid-plot is the mean of all aged pedigrees tested from the Chr 15 families, and the dotted lines represent two standard deviations from the mean. Arrows indicate outliers; all four homozygous mice tested from 92TNC were unable to maintain body temperature at 4 °C. In the case of 253 TNB, all three aged mice were hyperthermic throughout the test (0, 30, 60, and 90 min), with temperatures finally coming down to normal after 120 min in the cold. Note that 253 TNB also has low brain weight in aged animals, although n = only 2 thus far.

decreased numbers of proliferating cells in the rostral migratory stream and dentate gyrus as seen with anti-BrdU immunocytochemistry, and reduced numbers of anti-histone H3 positive cells in these areas. There also is an increase in ectopically placed histone H3-positive cells in regions that are not identified as normally proliferative including the striatum and various areas of cortex. An increase in GFAP immunoreactivity is also a hallmark of the aged brain, and this is particularly obvious in the thalamus. Finally, there is a variable but obvious drop out of Calbindin-positive Purkinje cells in the aged cerebellum. We are refining a set of quantitative measures of finer brain structure (cerebellar perimeter and area, cortical length and thickness, and area of the corpus callosum) that will provide a more in depth and quantitative view on brain structure.

Our screening further targets ocular structure and function. The first steps of vision comprise a multistep process involving a complex network of retinal neurons along with the supportive ocular structures that nourish and protect the retina. Multiple genetic mutations may have a late onset and therefore will not affect the quality of vision until the later stages of life. Other mutations have an early onset followed by progressive degeneration that may lead to loss of vision. In our analyses of aged mice, we have identified several pedigrees that may have a late onset occurrence of a disruption in Calbindin-positive cells. Although we have not tested the visual function of these mice, this immunohistochemical finding may indicate a disrupted ability of these pedigrees to process the visual stimuli presented to the eye. We have also identified several mutant pedigrees that appear to have progressive phenotypes that include an apparent loss of photoreceptor cells, loss of cell-specific marker proteins and loss of subretinal pigmentation that

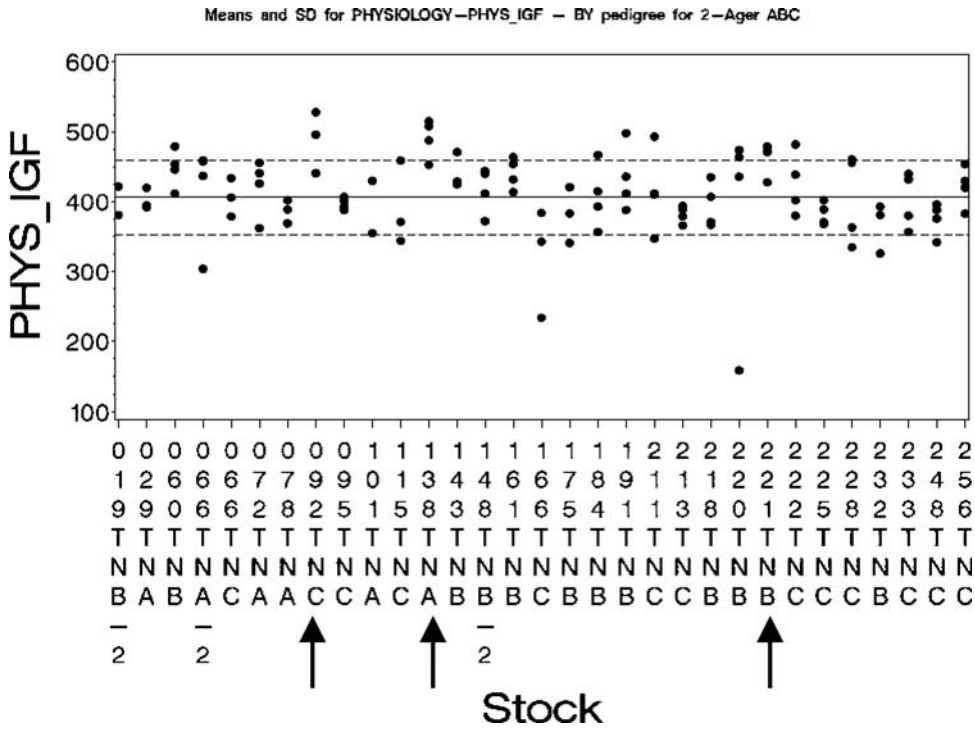

Figure 3. IGF-1 levels of 92TNC, 138TNA, and 221 TNB. SAS plot showing IGF-1 levels from distal chromosome 15 families TNA, TNB, and TNC. Pedigrees are listed across the bottom, with data points from individual animals of the pedigree arranged vertically above each pedigree. The solid line at mid-plot is the mean of all aged pedigrees tested from the Chr 15 families, and the dotted lines represent two standard deviations from the mean. Arrows indicate outliers showing elevated IGF-1 levels in all homozygotes tested from the pedigree. Note that 92TNC is an outlier for IGF-1 as well as for inability to maintain temperature upon cold challenge (Figure 2).

were not evident at 10 weeks of age. It must be stressed that the putant pedigrees for an ocular phenotype must be confirmed in additional mice prior to flagging of any pedigree for a mutant phenotype associated with aging.

Our statistical aim for this project is to identify, from among the majority of pedigrees that will be normal for these phenotypes amenable to high-throughput screening, the few pedigrees that may be abnormal due to a new ENU mutation. In all cases of the discovery (as opposed to the confirmation) phase of this screening, we compare the performance of four test-class mice from each pedigree with the performance of the test-class cohorts from all other pedigrees from that experiment (Table 1 outlines the experimental groups). There are, in the discovery phase, no formal controls other than the other pedigrees in the population, and no data are obtained from parental or grandparental mice. In the confirmation phase, which will come later for these potentially mutant aging pedigrees, statistically adequate numbers of mice from all possible genotypes will be tested to confirm both heritability and segregation patterns of each abnormal phenotype.

The goal of the statistical analysis of data from these primary screening tests, most of which are designed to identify abnormal phenotypes in apparently normal mice, is to identify pedigrees that are statistical outliers based on comparison to their particular test-class population. The age-onset behavioral, ocular, neuroanatomical, and longevity-associated phenotypes being assayed all likely behave as complex traits with inherent statistical variance resident in the tests. Inspection of the SAS plots in Figures 2–5 give an idea of the degree of variance we experience for the growth/stress tests; this variance is limited enough that we can call statistical outliers as potential mutants for retest. Since we have not yet re-aged any of the potentially mutant pedigrees for retest, we cannot yet calculate our success rate in confirming mutants on these tests. Our experience in testing in young mice (about eight weeks old) from

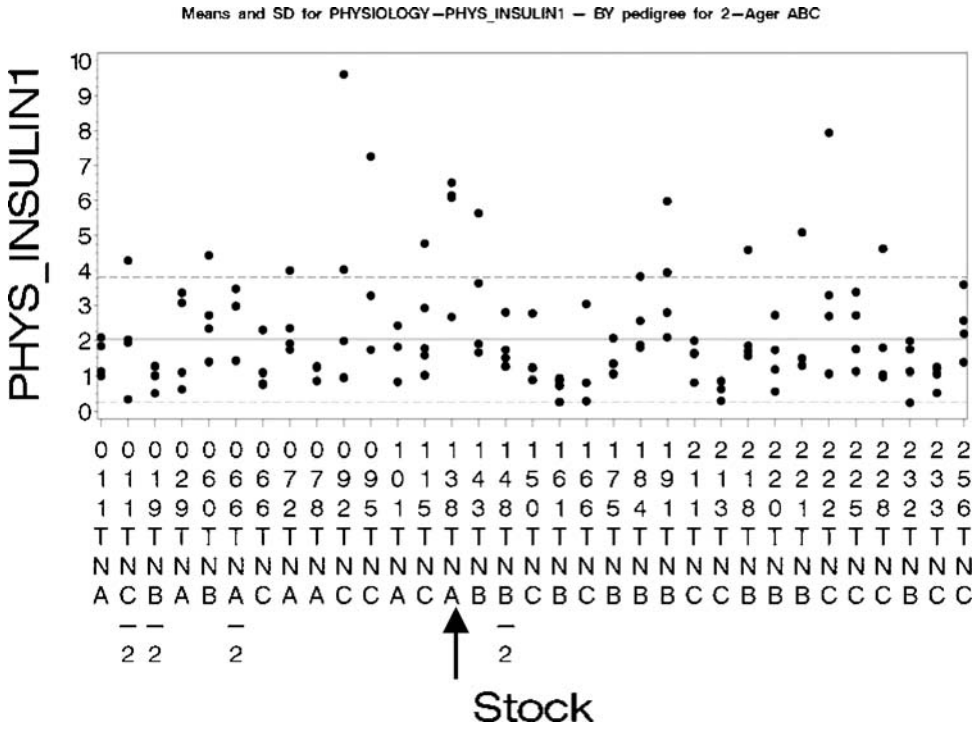

Figure 4. Insulin level of 138TNA (see also IGF-1 plot in Figure 2 for 138TNA). SAS plot showing insulin levels from distal chromosome 15 families TNA, TNB, and TNC. Pedigrees are listed across the bottom, with data points from individual animals of the pedigree arranged vertically above each pedigree. The solid line at mid-plot is the mean of all aged pedigrees tested from the Chr 15 families, and the dotted lines represent two standard deviations from the mean. Arrows indicate outliers showing elevated insulin levels in all homozygotes tested from the 138TNA, which is also an outlier for IGF-1 (Figure 3).

these same pedigrees on all of the behavior tests being used for the agers has taught us that when we have tested 20 or more test-class mice from two or more generations, we have been safe in designating the new phenotype as "mutant" and "heritable." Only retest of at least 20 aged mice from the next generation will tell us if these new age-onset phenotypes meet the "mutant" and "heritable" criteria.

Phenotype reliability, that is, the likelihood that phenotypes declared as potentially mutant will turn out to be heritable and to persist as detectable abnormalities in future generations, can be estimated using a new statistical tool in Mutrack at http://www2.tnmouse.org/mutrack/stats/heritability/php. This tool estimates our ability to detect the heritability of a particular phenotype, and is particularly useful if standard inbred strains have been phenotyped using a test with inherent variability. The tool is, however, also useful for assessing screening, like ours, in which only experimental animals have been tested. If one applies this tool to, for example, body weight taken for mice at 19 months of age, the heritability is 0.7 (SE 0.08), and we would expect an abnormal body-weight phenotype at this age to prove heritable as this is a complex trait. The acid test of phenotype reliability will occur, of course, only when these potential mutations have been confirmed experimentally.

High-throughput and robust screening protocols have been developed and validated for identifying age-onset disturbances of neurological function, and for growth and stress parameters that may predict longevity. Mice 28 months and older are available for additional or new screening assays that could be performed here in our colony. Thirteen potential mutants are or will be available to interested researchers. Each of these 13 has been or is being recovered as young animals for further testing and re-aging to confirm the stability and heritability of the new mutant phenotype.

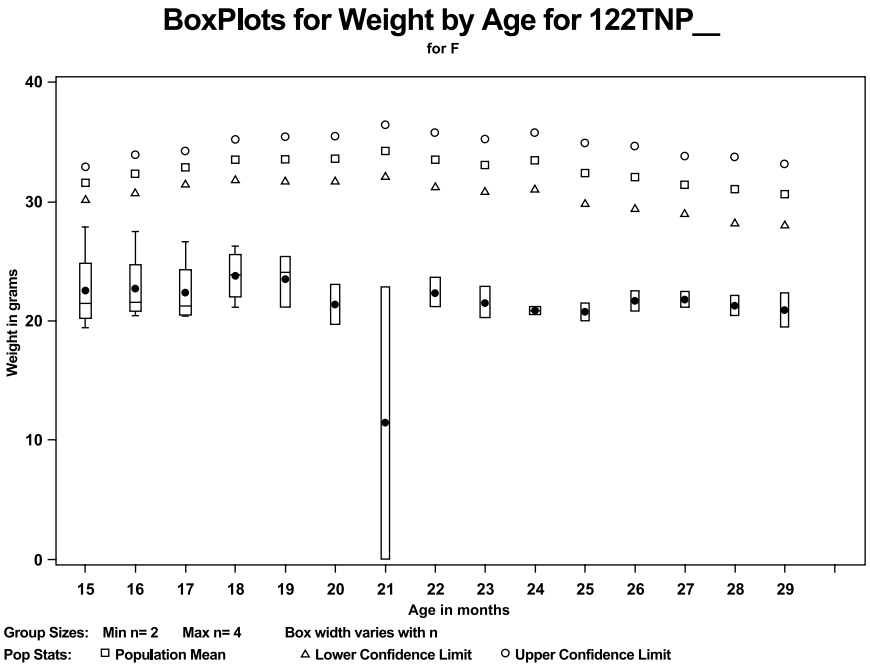

Figure 5. Low body weight of 122TNP females from 15–29 months of age. Box plot showing body weights of female mice from pedigree 122TNP at ages 15–29 months. Meanings of symbols are explained at the bottom of the plot.

Our screening targets for the extra-aged (to 28 months) mice are new mutations in genes responsible for growth and for stress resistance, since mutations in invertebrates and now in mice in growth and stress genes have been shown to be "longevity genes" (e.g., Holzenberger et al. 2003; Napoli et al. 2003, Migliaciccio et al. 1999). Several potential mutants are outliers in more than one screen; 92TNC, for example, shows an inability to maintain core temperature upon cold challenge, and also has higher than normal levels of IGF-1. 253TNB tends toward low brain weight in aged animals, and is also hyperthermic (Figure 2). 122TNP, with low body weight evidenced during aging (Figure 5), is also an outlier for nociception in young mice as determined by latency to lift paws from a 52 °C hot plate (data not shown). 138TNA shows increased levels of both insulin (Figure 4) and IGF-1 (Figure 3).

Because we are just beginning to understand the relationships between longevity, growth, and stress resistance, it is imperative that we identify the collection of genes and gene networks, likely preserved in evolution from yeast to humans, that mediate life span. Although we can use a gene-based, targeted approach to identifying and characterizing that set of genes it is imperative that we continue our search, via phenotype screening, for those novel genes whose role in longevity has not been realized or does not exist in lower eukaryotes. Once the genes responsible for these newly induced single-gene mutations have been mapped and cloned, we may discover new individual players in the longevity game and through them, identify the full set of cellular processes that govern life span.

References

de Haan G and Williams RW (2005) A genetic and genomic approach to identify longevity genes in mice. Mech Ageing Dev 126: 82–92

Holzenberger M, Dupont J, Ducos B, Leneuve P, Geloen A, Even PC, Cervera P and Le Bouc Y (2003) IGF-1 receptor regulates lifespan and resistance to oxidative stress in mice. Nature 421: 182–186

Kawase Y, Iwata T, Toyoda Y, Wakayama T, Yanagimachi R and Suzuki H (2001) Comparison of intracytoplasmic sperm injection for inbred and hybrid mice. Mol Reprod Dev 60: 74–78

Kimura Y and Yanagimachi R (1999) Intracytoplasmic sperm injection in the mouse. Biol Reprod 52: 709–720

Martin AC, Thornton JD, Liu J, Wang XF, Zuo J, Jablonski MM,

Chaum E, Zindy F and Skapek SX (2004) Pathogenesis of persistent hyperplastic primary vitreous in mice lacking the *Arf* tumor suppressor gene. Investig Ophthalmol Vis Sci 45: 3387–3396

Migliaciccio E, Giorgio M, Mele S, Pelicci G, Reboldi P, Pandolfi PP, Lanfrancone L and Pelicci PG (1999) The p66shc adaptor protein controls oxidative stress response and life span in mammals. Nature 402: 309–313

Napoli C, Martin-Padura I, de Nigris F, Giorgio M, Mansueto G, Somma P, Condorelli M, Sica G, De Rosa G and Pelicci P (2003) Deletion of the *p66Shc* longevity gene reduces systemic and tissue oxidative stress, vascular cell apoptosis, and early atherogenesis in mice fed a high-fat diet. Proc Natl Acad Sci USA 100: 2112–2116

Rinchik EM (2000) Developing genetic reagents to facilitate recovery, analysis, and maintenance of mouse mutations. Mamm Genome 11: 489–499

Russell WL, Kelly EM, Hunsicker PR, Bangham JW and Maddux SC (1979) Specific-locus test shows ethylnitrosourea to be the most potent mutagen in the mouse. Proc Natl Acad Sci USA 76: 5818–5819

Russell LB, Montgomery CS, Cacheiro NL and Johnson DK (1995) Complementation analyses for 45 mutations encompassing the pink-eyed dilution (*p*) locus of the mouse. Genetics 141: 1547–1562

Semenova E, Wang XF, Jablonski MM, Levorse J and Tilghman SM (2003) An engineered 800 kilobase deletion of *Uchl3* and *Lmo7* on mouse chromosome 14 causes defects in viability, postnatal growth and degeneration of muscle and retina. Hum Mol Genet 12: 1301–1312

Szczygiel MA, Kusakabe H, Yanagimachi R and Whittingham DG (2002) Intracytoplasmic sperm injection is more efficient than *in vitro* fertilization for generating mouse embryos from cryo-preserved spermatozoa. Biol Reprod 67: 1278– 1284

The Complex Trait Consortium (2004) The Collaborative Cross, a community resource for the genetic analysis of complex traits. Nat Genet 36: 1–4

Vogel G (2003) Scientists dream of 1001 complex mice. Science 301: 456–457

Williams RW (1999) A chromosome-specific recessive mutagenesis screen suitable for detecting mutations with subtle effects. Mamm Genome 10: 734–738